1   **Expression of retrotransposons contributes to aging in *Drosophila***

2

3   Blair K. Schneider[1], Shixiang Sun[1], Moonsook Lee[1], Wenge Li[2], Nicholas Skvir[3], Nicola

4   Neretti[3], Jan Vijg[1,4], and Julie Secombe[1,5,6]

5

6   [1] Department of Genetics, Albert Einstein College of Medicine, Bronx, New York, United

7   States of America.

8

9   [2] Department of Cell Biology, Albert Einstein College of Medicine, Bronx, New York,

10   United States of America.

11

12   [3] Department of Molecular biology, Cell biology and Biochemistry, Brown University,

13   Providence, Rhode Island, United States of America.

14

15   [4] Department of Ophthalmology and Visual Sciences, Albert Einstein College of

16   Medicine, Bronx, New York, United States of America.

17

18   [5] Dominick P. Purpura Department of Neuroscience, Albert Einstein College of

19   Medicine, Bronx, New York, United States of America.

20

21   [6] corresponding author: julie.secombe@einsteinmed.edu (JS)

22   Running title: Expression of transposons contributes to aging

23   Key words: Lifespan extension, aging, retrotransposon, 412, Roo, Retrofind.

Abstract

24

25   Retrotransposons are a class of transposable elements capable of self-replication and

26   insertion into new genomic locations. Across species, the mobilization of

27   retrotransposons in somatic cells has been suggested to contribute to the cell and

28   tissue functional decline that occurs during aging. Retrotransposon expression generally

29   increases with age, and *de novo* insertions have been observed to occur during

30   tumorigenesis. However, the extent to which new retrotransposon insertions occur

31   during normal aging and their effect on cellular and animal function remains

32   understudied. Here we use a single nucleus whole genome sequencing approach in

33   *Drosophila* to directly test whether transposon insertions increase with age in somatic

34   cells. Analyses of nuclei from thoraces and indirect flight muscles using a newly

35   developed pipeline, Retrofind, revealed no significant increase in the number of

36   transposon insertions with age. Despite this, reducing the expression of two different

37   retrotransposons, *412* and *Roo*, extends lifespan, without increasing stress resistance.

38   This suggests a key role for transposon expression and not insertion in regulating

39   longevity. Transcriptomic analyses revealed similar changes to gene expression in *412*

40   and *Roo* knockdown flies and highlighted potential changes to genes involved in

41   proteolysis and immune function as potential contributors to the observed changes in

42   longevity. Combined, our data show a clear link between retrotransposon expression

43   and aging.

44

Author Summary

46   With the onset of modern medicine, the average age of the population has significantly

47   increased, leading to more individuals living with chronic health issues. Rather than

48   treat each age-associated disorder individually, one approach to target multiple health

49   concerns simultaneously might to be target aging itself. Genomic instability is a hallmark

50   of aging cells that has been proposed to be a key contributor to age-associated cellular

51   decline. Transposons are mobile genetic elements capable of inserting into new

52   genomic locations, thus having the potential to increase genomic instability. Consistent

53   with this, transposon expression generally increases with age. However, the extent to

54   which transposon insertions accumulate to disrupt the genome of cells within aging

55   individuals has remained an open question. We specifically answer this through single

56   cell whole genome sequencing and find that transposon insertions do not increase with

57   age. Even though insertions did not increase, the expression of transposons is linked to

58   aging, as reducing the expression of individual transposons extended lifespan.

59   Transcriptome studies of these long-lived flies revealed increased expression of genes

60   linked to proteolysis genes and to functioning of the immune system. Our study

61   therefore establishes transposon expression, and not insertion, as a critical contributor

62   to animal aging.

63

64   **Introduction**

65   Across species, aging is associated with functional decline and an increased

66   likelihood of one or more disorders that adversely affect quality of life (1, 2). Driving the

67   changes that occur at the whole animal level are a range of alterations to cellular

68   function. One hallmark of aging is genomic instability, in which the accumulation of

69 mutations can alter critical gene expression programs and impact cell division by

70 promoting tumor formation or by increasing cellular senescence (3, 4). One predicted

71 genetic contributor to aging is the expression and mobilization of transposable elements

72 (TEs) in somatic cells. TEs are abundant, comprising ~45-50% of the human, ~37% of

73 the mouse, and ~20% of the *Drosophila* genomes (5-9). While the specific TEs found in

74 each animal species are distinct, TEs are a universal feature of eukaryotic genomes

75 whose expression generally increases with age (10-12). This increased expression

76 relates to Class 1 transposons, also known as retrotransposons (RTs), that replicate

77 using an RNA intermediate or a 'copy, paste' mechanism (12). RTs are therefore able to

78 increase their genomic copy number over time, which gives them a high mutagenic

79 potential. In contrast, class 2 transposons (DNA transposons) mobilize by excising

80 themselves in a 'cut, paste' mechanism, so their total number does not increase over

81 time (12) and less is known about their expression with respect to aging. However, the

82 precise role that TEs play in driving age-related phenotypes remains an open question.

83

84   The most obvious consequence of TE expression with age is the potential to cause

85 genomic instability through insertional mutagenesis and/or the creation of

86 insertions/deletions because of the double-stranded DNA breaks that are needed for TE

87 reinsertion (12, 13). In addition, cDNA generated as an intermediate during RT

88 mobilization can activate the immune response and lead to chronic inflammation in

89 mammals (14-16). Consistent with their potential for interfering with cellular function,

90 several mechanisms that are conserved across species have evolved to limit the

91 expression of transposons. For example, many transposons in the genome are

92   contained within constitutive heterochromatin, which is largely transcriptionally silent (3,

93   9, 17-20). For those elements inserted within euchromatin, RT expression is regulated

94   post transcriptionally via the siRNA pathway that degrades double-stranded RNA

95   complexes (21, 22). Further supporting a role for heterochromatin and RNAi in

96   repressing TE's influence on aging, modulating the activity of either of these pathways

97   can alter lifespan. For example, reducing the expression of the heterochromatin

98   component *Lamin B* or components of RNAi-mediated TE silencing machinery

99   decreases lifespan in *Drosophila* (11, 20). Conversely, increasing expression of the

100   heterochromatin-promoting histone methyltransferase, *su(var)3-9*, or the activity of the

101   RNAi pathway increases lifespan (20, 23, 24). It is, however, notable that

102   heterochromatin and the RNAi pathway are not specific to the repression of TEs, which

103   complicates the interpretation of the changes to lifespan observed. More direct evidence

104   supporting a link between TE activation and aging has come from the use of reverse

105   transcriptase inhibitor drugs that broadly inhibit the ability of RTs to replicate. For

106   example, *Drosophila* fed nucleoside reverse transcriptase inhibitors (NRTIs) have an

107   increased lifespan compared to controls (25). This is also observed in mice, where

108   NRTI treatment attenuates the shortened lifespan caused by loss of *SIRT6*, a known

109   repressor of *LINE1 (L1)* elements (14).

110

111   The key to understanding the link between TEs and aging is the extent to which their

112   expression leads to new insertions. Analyses of the TE, *mdg4* (formerly known as

113   *Gypsy*), in the adult *Drosophila* brain and fat body using a reporter revealed an increase

114   in the number of insertions with age (20, 23, 26). However, expanding these findings to

5

115 endogenous TEs has been challenging, as each somatic cell contains a unique set of

116 insertions which are difficult to detect using bulk whole genome sequencing

117 approaches. One approach to address this has been to develop bioinformatic tools to

118 detect TE insertions more accurately, for example, by using TE junction and target site

119 duplication data. When applied to bulk whole genome sequencing (WGS), this approach

120 can detect an age-associated increase in TE insertion number in fly strains with reduced

121 RNAi pathway activity and in clonally expanded tumors, but not in wild-type animals (24,

122 27). New insertions can also be accurately identified using long-read sequencing of bulk

123 DNA as whole elements are detected rather than breakpoints (24, 27). While a small

124 number of *de novo* insertions were observed using this technique, it was difficult to

125 determine how frequently TEs mobilized. While technologies to detect new TE

126 insertions in somatic cells have become more robust using bulk sequencing

127 approaches, the frequency of new TE insertions within individual somatic cells during

128 aging remains unknown.

129

130   To understand the extent to which TEs mobilized during aging, we took a single

131 nucleus whole genome sequencing (WGS) approach using a new pipeline called

132 Retrofind, that allows us to accurately define the insertional position and load per cell.

133 Using nuclei isolated from adult thoraces or indirect flight muscles (IFMs), we found that

134 the number of TE insertions does not increase with age. However, reducing the

135 expression of two individual TEs, *412* and *Roo*, led to lifespan extension. This suggests

136 a key role for the expression, and not insertion, of TEs impacting lifespan. This

137 increased lifespan did not correlate with improved stress resistance or other health

138   improvements traditionally associated with longer life. Transcriptomic studies of long-

139   lived TE knockdown flies revealed that the expression of genes involved in proteolysis

140   were upregulated, including the *Jonah* family of genes that encode serine hydrolases.

141   Additionally, antimicrobial peptides (AMPs), the downstream products of activation of

142   the *Drosophila* innate immune system that is similar to mammalian inflammation, were

143   dysregulated in knockdown animals. Overall, our studies show that TE expression and

144   not insertion likely contributes to aging, potentially through regulation of the *Jonah*

145   genes and immunity.

146

147   **Results**

148   **TE insertions do not increase with age**

149   To identify *de novo* TE insertions, we used a single nucleus whole genome

150   sequencing approach (Fig 1A). Using this methodology, new insertions are represented

151   in approximately half of the reads in each nucleus, facilitating robust detection. We

152   carried out our studies using the well characterized w^{1118} strain that shows a typical

153   lifespan and is often used a wild-type control strain (Fig 1A)(24, 28). To distinguish new

154   insertions that occur with age from preexisting ones within the germline genome, we

155   defined the TE landscape in the w^{1118} strain by carrying out bulk sequencing from

156   pooled young thoraces to a total depth of 157x coverage. Sequencing data was

157   analyzed using a newly developed in-house TE detection pipeline called RetroFind, in

158   addition to a published pipeline that has successfully detected somatic insertions in

159   clonally expanded tumors, so serves as independent validation (27). New TE insertions

160   were identified by similar criteria for each pipeline by detecting both split and discordant

161   reads of evidence from paired-end sequencing data. Additionally, newly called insertion

162   sites in the germline genome needed to possess the target site duplication that occurs

163   because of the double stranded breaks made by the TE-encoded integrase. A total of

164   871 TE insertions unique to w^{1118} relative to the *dm6* reference genome were detected

165   by the two pipelines, with 505 being detected by both (Fig 1B, S1 Table). We consider

166   these to be high confidence insertions. TE insertions identified in w^{1118} were primarily

167   within intronic and intergenic regions and were largely excluded from promoters (+/- 100

168   base pairs of the transcription start site) and coding sequences (CDS) where they might

169   disrupt gene function (Fig 1C).

170

171   To determine if the number of TE insertions increased with age in somatic cells, we

172   isolated and amplified genomic DNA from 21 individual nuclei from thoraces of young (5

173   days old) and from old (50 days old) flies (Fig 1A). Whole genome sequencing (WGS) of

174   these 42 nuclei revealed an average 317x coverage of the genome for nuclei from

175   young thoraces and 354x for nuclei from old thoraces. To confirm our ability to map TEs

176   in individual nuclei, we looked for the 505 high confidence TE insertions detected from

177   sequencing bulk genomic DNA. Confirming a robust ability to detect TEs, we find an

178   average of 90% of high confidence insertions in nuclei from young animals and 94%

179   from old animals (Fig 1D). While it is notable that more of the known w^{1118} insertions

180   were detected in nuclei from old animals, this likely reflects the higher sequencing depth

181   observed from these samples.

182

8

183   To identify *de novo* insertions, we used Retrofind and the published pipeline to

184   analyze the sequencing data for each nucleus, with unique insertions detected by both

185   pipelines being deemed high confidence (27). This revealed that 57% and 76% of nuclei

186   from young and old animals, respectively, did not have any new TE insertions (Fig 1E).

187   A total of 15 new insertions were found across 9 nuclei from young animals and 4 from

188   old. A maximum of two insertions was detected in any individual nucleus. Each of the 15

189   *de novo* TE insertions detected was visually confirmed using Integrated Genome Viewer

190   (IGV), similar to previous studies (27). Like existing TE insertions within the genome,

191   new insertions occurred primarily in non-coding regions of the genome (Fig 1F). Most of

192   the new insertions were observed in nuclei from young flies, and all the insertions

193   observed in old flies, were the *hobo* element (also known as the *H-element*) (S2 Table).

194   This DNA terminal inverted repeat transposon is an evolutionarily recent addition to the

195   *Drosophila* genome that is known to be active (29). In addition, the long terminal repeat

196   (LTR) retrotransposon *HMS-Beagle* and the DNA *S terminal inverted repeat element*

197   showed a new single insertion in the somatic genome, each in a single nucleus from

198   young animals. Based on these data, we tested whether the w^{1118} strain shows

199   increased TE expression with age. Using qPCR, we find that the expression of a subset

200   of TEs increases expression with age (Fig 1G). For instance, the TEs *Gypsy12* and

201   *Copia* that have been previously shown to increase their expression with age in other

202   tissues such as the fat body (11). The expression of other elements did not change with

203   age, such as *412* and *Roo*, and some showed decreased expression, such as *297* (Fig

204   1G). Thus, increased expression of TEs with age does correlate with additional

205   insertional events.

206

207   Because our single nuclei were isolated from thoraces, they likely represent several

208   different cell types, possibly obscuring an increase in TEs that might be observed by

209   analyzing a single tissue. We therefore also purified nuclei from indirect flight muscles

210   (IFMs), which are a major muscle group in the thorax that show age-associated decline

211   (30-33). To purify IFM nuclei, they were labeled by a nuclear membrane localized GFP

212   (UAS-GFP:KASH) using UH3-Gal4 (UH3>GFP:KASH; Fig 2A) (34). Individual GFP

213   positive nuclei from dissected thoraces were isolated by fluorescence-activated cell

214   sorting and whole genome amplified in a similar manner to our analyses of thoracic

215   nuclei. Unamplified, bulk DNA from the abdomen and head regions of the same flies

216   were sequenced to a total of 443x coverage to exclude strain-specific TE insertions.

217   Sequencing of the individual nuclei revealed an average of 64x coverage from young

218   nuclei and 115x from old. Like our findings using nuclei from thoraces, analyses of six

219   and seven IFM nuclei from young and old flies, respectively, revealed no significant

220   increase in TE insertions with age (Fig 2B). Approximately half of nuclei examined had

221   no new insertions and the small number that were observed were inserted into

222   intergenic or intronic sequences (Fig 2C). These data show that TE insertions do not

223   increase significantly during aging in cells of the thorax or IFMs.

224

225   **Reduced expression of individual retrotransposons extends lifespan**

226   While no increase in TE insertions were observed during adulthood, the expression

227   of these elements could impact cell function, thereby altering lifespan. For this reason,

228   we examined the effect of attenuating retrotransposon expression. We chose to focus

229   initially on the retrotransposon *412*, which is part of the *gypsy* super-family of LTR

230   elements that has been previously shown to be stable in the germline (35). Consistent

231   with this, we did not observe any new *412* insertions in w^{1118} compared to the

232   sequenced strain (S1 Table). Like most RTs, *412* is multi-copy within the genome,

233   having 36 copies in total, 24 of which are full length (36). We therefore used a

234   knockdown approach to reduce the expression of *412* to assess the effect on life- and

235   healthspan. To do this, we generated two UAS-regulated short hairpin transgenes,

236   412#1, and 412#2, in addition to a control construct expressing a shRNA predicted not

237   target any mRNAs (control). Driving the expression of UAS-shRNA transgenes targeting

238   *412* with the ubiquitous Actin5C-Gal4 (Act5C>shRNA) driver led to a ~2-fold reduction

239   in *412* mRNA levels (Fig 3A). *412* knockdown flies completed metamorphosis normally

240   and were grossly morphology normal (S1 Fig). Quantifying the lifespan of these animals

241   revealed significantly extended median and maximum lifespan compared to controls

242   (Fig 3B-D).

243

244   To confirm the lifespan extension caused by RNAi-mediated knockdown of *412*, we

245   additionally used CRISPR interference (CRISPRi) to reduce expression of this TE. To

246   do this, we generated a UAS transgene encoding an enzymatically dead Cas9 protein

247   fused to the *KRAB* transcriptional repressor (UAS-dCas9:KRAB). dCas9:KRAB was

248   targeted to the *412* LTR enhancer/promoter region using a transgene expressing a

249   guide RNA (gRNA) under the control of the ubiquitously expressed, *U6* promoter

250   (412gRNA). As a control, we generated control non-targeted gRNA (control gRNA).

251   CRISPRi was carried out by crossing Act5C>dCas9:KRAB and 412gRNA flies, which

252 led to a 1.7-fold reduction in 412 mRNA levels (Fig 3E). In contrast to 412 knockdown

253 adult flies that were indistinguishable from controls, 412gRNA CRISPRi flies were 7%

254 heavier than control gRNA flies although they were morphologically normal (S1 Fig).

255 Mirroring our shRNA results, 412 gRNA-expressing flies showed extended median and

256 maximum lifespan compared to control gRNA-expressing flies (Fig 3F-H). Reducing the

257 expression of a single RT is therefore sufficient to extend lifespan.

258

259   To test whether changes in lifespan were specific to *412*, we reduced the expression

260 of another RT that showed 112 new insertions in w^{1118} compared to the annotated

261 *Drosophila* genome (S1 Table). Driving the expression of a UAS-shRNA transgene

262 targeting *Roo* using Act5C-Gal4 led to a ~2-fold reduction in mRNA levels and did not

263 adversely affect ability of animals to complete metamorphosis or their gross morphology

264 (Fig 3I; S1 Fig). Quantifying the lifespan of these animals revealed a significantly

265 extended median and maximum lifespan compared to control animals (Fig 3J-L). The

266 expression of *412* and *Roo* therefore both contribute to aging.

267

268 **Long-lived 412 or Roo knockdown flies do not show improved locomotion or**

269 **stress resistance.**

270   Extension of longevity can be associated with improved healthspan, which can be

271 measured as a delay in the onset of age-associated phenotypes. For example, long-

272 lived fly strains, such as those with reduced insulin signaling, show increased resistance

273 to starvation and oxidative stress (37). Additionally, progeroid flies have an accelerated

274 decline in locomotor activity with age (38). We therefore tested the extent to which flies

275   with reduced expression of *412* or *Roo* showed improvements in locomotion and/or

276   resistance to a range of stress conditions. One classic indicator of age-associated

277   decline is a reduced locomotion, which can be quantified using a negative geotaxis

278   assay. This assay takes advantage of an innate response whereby flies move against

279   gravity by climbing to the top of a vial after being tapped to the bottom (39). Young,

280   healthy, flies quickly climb to the top third of the vial while fewer older flies climb this

281   distance. As expected, locomotor ability declined with age across genotypes, with those

282   in midlife (18 days old) and old age (40 days old) showing an attenuated negative

283   geotaxis response than young flies (5 days old) (S2 Fig). Midlife flies also have more

284   locomotion when compared to old age flies (S2 Fig). At all ages tested, *412* knockdown

285   flies displayed locomotor capacity that was either indistinguishable or worse (412#1)

286   than control animals (412#2) (Fig 4A and S2 Fig). Similarly, the locomotor capacity of

287   *Roo* knockdown animals was not different than control animals (Fig 4A).

288

289   To assess whether reduced RT expression altered resistance to oxidative stress, we

290   treated ubiquitous *412* or *Roo* knock down flies with paraquat and quantified survival

291   compared to control flies. This revealed that the two *412* shRNA transgenes behaved

292   differently from each other, with 412#2 showing no change to survival and 412#1 having

293   slightly reduced resistance to oxidative stress (Fig 4B). *Roo* knockdown animals

294   showed no change resistance to oxidative stress compared to control animals (Fig 4B).

295   We additionally tested survival in response to endoplasmic reticulum (ER) stress

296   through treatment with the antibiotic tunicamycin (40), starvation, and thermal stress

297   (cold and heat). None of these treatments led to a consistent change in survival for *412*

298   or *Roo* knockdown flies except starvation, where both *412* knockdowns showed

299   increased sensitivity (Fig4C-F). An additional corollary to increased lifespan is a decline

300   in fertility (41). We therefore quantified fecundity of *412* and *Roo* knockdown flies by

301   counting the number of eggs laid per day and found no significant difference (Fig 4G).

302   Nor was the fertility of *412* or *Roo* knockdown animals altered, as the number of adult

303   flies produced from those eggs was indistinguishable from controls (Fig 4H). Combined,

304   these assays show that reducing *412* or *Roo* expression does not improve standard

305   assays of health and/or stress resistance that might be expected in these long-lived

306   flies.

307

308   **TE knockdown affects genes linked to proteolysis and immunity**

309   To gain insight into the cellular changes caused by reduced TE expression, we

310   performed RNA-seq on thoraces of Act>shRNA animals at mid-life (day 20). We chose

311   mid-life as others have seen changes to age-associated phenotypes at this time point

312   (20, 38). 332 differentially expressed genes (DEGs) were identified in *412* knockdown

313   animals compared to control shRNA expressing flies using a 5% false discovery rate

314   (FDR) cutoff. 212 of these genes were upregulated while 120 were downregulated and

315   averaged a log2 fold change of 2.5 and 1.5, respectively (Fig 5A; S3 Table). Functional

316   analyses of upregulated genes using GO DAVID revealed significant enrichment in the

317   single gene ontology (GO) category of proteolysis using a 1% FDR (42, 43). Many of

318   these genes were members of the Jonah (Jon) family of serine proteases, including

319   *Jonah 25Bi-iii, Jonah 44E, Jonah 65Aiii, Jonah 65Aiv, Jonah 74E,* and *Jonah 99Ci-iii*

14

320 (S5 Table) (42, 43). Similar GO analyses of downregulated genes did not reveal any

321 significantly enriched categories using an FDR of 1%.

322

323   To determine the extent to which knockdown of *Roo* led to similar changes to gene

324 expression as *412*, we carried out RNA-seq analyses using thoraces of ubiquitous *Roo*

325 knockdown flies. 344 genes were found to be differentially expressed in *Roo* knockdown

326 animals, 236 of which were upregulated average and 108 were down compared to

327 control animals (5% FDR; Fig 5B; S4 Table). As with knockdown of *412*, the changes to

328 gene expression in response to reduced *Roo* expression were relatively small,

329 averaging 1.1 and 1.3 log2 fold change for up- and downregulated genes, respectively.

330 Interestingly, upregulated genes were enriched for the same proteolysis GO term as

331 was observed in *412* knockdown animals (42, 43) (1% FDR cutoff; S6 Table). No GO

332 terms were significantly enriched among the downregulated genes.

333

334   Based on the identification of the same GO term in *412* and *Roo* knockdown

335 datasets, we compared the transcriptional changes of these two strains. This revealed

336 97 genes common to both datasets, a majority of which behaved similarly (r=0.9461;

337 p<0.0001; Fig 5C). These genes were enriched for the single GO term of proteolysis

338 (42, 43) (1% FDR cutoff; S7 Table). To understand the relationship between genes

339 observed to be dysregulated within the proteolysis GO category, we used STRING,

340 which revealed a distinct interaction node mainly based on co-expression and co-

341 occurrence (Fig 5D) (44). The *Jon* genes, a family of serine proteases, were at the

342 center of this node (45). Two thirds of the genes affected by *412* and *Roo* knockdown

15

343   were upregulated in knockdown flies, including all of the genes within the proteolysis

344   category (Fig 5E). While little is known about the Jonah proteins, their expression

345   appears to be primarily in the gut, where they are assumed to aid in digestion (45).

346   However, expression of the *Jon* genes has also been linked with changes to the

347   immune deficient (IMD) and Toll immunity pathways, which have previously been

348   associated with lifespan regulation (46-48). Consistent with this, the expression of

349   antimicrobial peptides (AMPs) that are downstream of the IMD and Toll pathways are

350   affected in *412* or *Roo* knockdown flies, with several *Drosomycins* (e.g., *Drsl2*, *Drsl3*,

351   *Drsl5*) significantly downregulated and *Attacin-A* (*AttA*) being significantly upregulated

352   (Fig 5F). Overall, our data suggest that TEs such as *412* and *Roo* alter the expression

353   of genes related to proteolysis regulation and the immune system to influence longevity.

354

355   **Discussion**

356   In this study we find that there is no significant increase in TE mobilization with

357   age in *Drosophila*, indicating that they have a robust mechanism for preventing *de novo*

358   TE insertions in somatic cells. Based on the observation that reduced activity of the

359   RNAi pathway leads to an increase in TE insertions with age, this mechanism is likely a

360   key means of limiting *de novo* TE insertions during normal aging (24). By combining a

361   single nucleus whole genome sequencing approach with analyses using two pipelines,

362   we are confident that new insertions would have been detected if present. Prior to our

363   study, the most compelling data indicating increased TE insertions with age in wild-type

364   animals came from use of a TE reporter transgene and sequencing of bulk DNA

365   samples (24, 27, 49). Use of a fluorescent reporter for the RT *mdg4* revealed age-

16

366   associated *de novo* insertions in cells of the adult brain and fat body, although the

367   frequency was low (23, 26). In addition, examining the insertional proficiency of all TEs

368   through long-read sequencing of pooled adult brains or midguts showed new insertions

369   by several different elements, including *mdg4* and *Roo* (27). Like the *mdg4* reporter

370   data, the number of new insertions detected using this approach was low, averaging

371   less than one new integration event per individual (27). Because both approaches

372   identified new insertions, it is possible that TEs are more highly expressed in the gut

373   and brain than cells of the thorax, allowing some insertions to occur during aging in

374   these tissues. Alternatively, given the low frequency of new TE insertions that were

375   observed, it is more likely that these published data are congruent with our study. Based

376   on the rate of transposition observed, our sequencing analyses of 42 thoracic nuclei (21

377   from young flies and 21 from old) was unlikely to be sufficient to detect new insertions.

378   Consistent with our data that endogenous expression of TEs does not necessary lead to

379   new insertions, overexpression of *mdg4* does not increase the number of genomic

380   copies of this element (50). We therefore suggest that new TE insertions are unlikely to

381   be a key driver of cell and tissue dysfunction that occurs during normal aging.

382   Interestingly, this contrasts with disorders such as cancer where there is clear evidence

383   from mammalian cells and flies that TE insertions are a frequent occurrence that likely

384   impact disease severity (27, 51-53).

385

386   Previous functional evidence supporting TE mobilization playing a role in aging

387   has come from the pharmaceutical approach of using RT inhibitors, with

388   phosphonoformic acid (PFA) or dideoxyinosine (ddI) and Lamivudine (3TC) or

389   Stavudine (d4T) treatment extending lifespan in *Drosophila* and mice, respectively (14,

390   25). NRTIs are well-established to block retrotransposon replication thereby preventing

391   RT reinsertion (14). However, RT inhibitor treatment can additionally decrease RNA

392   levels of the *L1* element in human cells, thus the effect of these drugs may not be

393   limited to restricting mobilization (49). If NTRIs exert similar effects in flies, the extended

394   lifespan seen using these drugs could be due to reduced expression of some or all TEs,

395   rather than changes to replicative capacity. These data, like ours showing that TE

396   knockdown affects lifespan without increasing mobilization, suggest that the presence of

397   TE mRNA may be generally detrimental to cell and animal function.

398

399   Because of their similarity to retroviruses, cytosolic DNA intermediates produced

400   by RTs can trigger the activity of the immune system (14-16, 54). In human cells, *L1*

401   retrotransposon expression induces the interferon beta (*IFNβ*) inflammatory response

402   (15, 16). This can lead to chronic inflammation (inflammaging), which is common in

403   aged individuals and is associated with cellular senescence (16). In mammals,

404   recognition of cytosolic RT DNA by *cGAS/STING* triggers the *NFκB* pathway and the

405   *IFNβ* inflammatory response (14, 54). *Drosophila* does not have adaptive immunity, but

406   many proteins that comprise the innate immune response are homologous to those that

407   regulate the mammalian inflammatory response (54). In *Drosophila,* STING activates

408   the *NFκB* homolog *Relish* to activate the immune defective (IMD) pathway and the

409   expression of AMPs (54). This functions in parallel to the Toll pathway that acts through

410   *Dorsal-related immunity factor* (*Dif*), another *NFκB* homolog, to activate the production

411   of AMPs (55-57). We did not find the expression of components of the upstream

18

412   components of the IMD and Toll pathways to be altered in *412* or *Roo* knockdown

413   animals. However, several *Drosomycin* genes that encode AMPs downstream of the

414   Toll pathway activation were downregulated upon TE knockdown. Lowering the

415   expression of AMPs extends lifespan (58), suggesting that this may contribute to the

416   lifespan changes seen in TE knockdown flies. While the mechanism by which *412* or

417   *Roo* knockdown alters the expression of AMP genes remains to be determined, it may

418   be linked to the upregulation of genes involved in proteolysis. In particular, genes of the

419   *Jonah* serine hydrolase family are activated upon RNA viral infection and can influence

420   the expression of *Drosomycins*, although the mechanism for this is unknown (47, 48).

421   Jon proteins have a conserved function as their mammalian homolog, *Chymotrypsin like*

422   (*CTRL*), is also involved in proteolysis within the gut (45, 59-62). Recently, a

423   chymotrypsin/trypsin fusion protease has been utilized as a treatment for inflammation

424   and to promote wound healing (63), suggesting a conserved link between these serine

425   proteases and inflammation. We therefore hypothesize that the upregulation of the

426   *Jonah* genes could dampen the immune system, and this could contribute to the

427   extension of lifespan seen in animals with reduced expression of TEs.

428

429   Increased lifespan often coincides with improved stress resistance or other

430   markers of health as illustrated by the insulin mutant and progeroid flies showing

431   changes to oxidative stress and starvation and locomotion, respectively (37, 38). In

432   contrast, knockdown of *412* or *Roo* increased lifespan without promoting observable

433   stress resistance or delaying the onset of age-associated changes such as decreased

434   mobility. Previous studies in *Drosophila* examining changes to heterochromatic and

19

435   RNAi pathways to modulate TE activity did not examine these classic stress assays (11,

436   23). Thus, it is possible that TE expression-induced changes to lifespan occur without

437   altering stress resistance, effectively uncoupling life- and healthspan. Defining the

438   precise links between *412*, *Roo* and other TEs and their effect on cellular and organism

439   function during aging will require additional genetic and molecular studies to elucidate

440   the links between the *Jonah* genes, immunity, and aging.

441

442   **Materials and methods**

443   **Fly strains**

444   The following fly stocks were obtained from Bloomington Drosophila Stock Center:

445   Act5C-Gal4 (BL #3954), w^{1118} (BL#5905), UAS-dcas9-VPR (BL#67062). UH3-Gal4 was

446   a gift from the Sparrow lab (Singh et al., 2014). UAS-shRNAs were generated according

447   to the TRiP protocol using the pVALIUM20 vector (Addgene) (64). shRNA primers are

448   listed in the primers table and were designed using the Designer of Small Interfering

449   RNA webtool (65). UAS-shRNAs were inserted into the attP site at 86F (BL #24749) by

450   BestGene. gRNA flies for CRISPRi were generated using the protocol from CRIPR fly

451   design (66-72). The pCFD3 vector (Addgene) was used to insert a gRNA downstream

452   of the U6:3 promoter, allowing for ubiquitous expression of the gRNA. gRNA transgenes

453   were inserted into the attP site at 86F (BL #24749) by BestGene. UAS-dcas9:KRAB

454   flies were created by In-Fusion® cloning system (Takara) using the pUAST-attB from

455   the Drosophila Genomics Resource Center (# 1419) and dCas9-KRAB (Addgene

456   SID4X-dCas9-KRAB; #106399). The primers are listed in the S8 Table and the PCR

457   amplifications were performed using the CloneAmp™ HiFi PCR Premix (Takara). The

20

458   pUAST-dCas9-KRAB plasmid was recombined into the attP site attP40 (BL #24749) by

459   BestGene.

460

461   **Fly care**

462   Fly food contained 80g malt extract, 65g cornmeal, 22g molasses, 18g yeast, 9g agar,

463   2.3g methyl para-benzoic acid and 6.35ml propionic acid per liter. Flies were kept at

464   25℃ with a 12-hour light/dark cycle and 50% humidity. Day of eclosion is defined as day

465   zero in all analyses. Adults were collected 2 days after the first flies eclosed, allowed to

466   mate for a day, sorted by sex and allowed to age to the specified time point. Flies were

467   kept at a density of 25 or less per vial. Flies were transferred to a new vial of food twice

468   a week until they reached the desired age for the experiment. All of these studies used

469   female flies.

470

471   **RNA-seq**

472   Triplicate samples of 20 thoraces from adults were collected at day 20 from

473   Act5C>shRNA (Control, 412#1, and Roo) and frozen at -80℃. RNA was extracted using

474   TRIzol (Invitrogen) and sent to Novogene for quality assessment, library preparation,

475   sequencing, and differential expression analysis. Sequencing was performed on using

476   an Illumina platform with a sequencing by synthesis (SBS) method. HISAT2 was used

477   to map the reads to the *Drosophila* genome (*dm6*), Novogene calculated the read

478   counts and FPKM (fragments per kilobase of transcript per million base pairs

479   sequenced) values and then used DESeq2 was used to perform differential expression

480   analysis (73). DAVID was used to obtain gene ontology (GO) terms (42, 43). String was

481 used to observe protein interactions of the enriched gene products (44). The data

482 discussed in this publication have been deposited in NCBI's Gene Expression Omnibus

483 (74) and are accessible through GEO Series accession number GSE207160.

484

485 **qPCR**

486 TRIzol was used to extract total RNA from 5 whole adult flies quantification of

487 knockdown efficiency and heads and thoraces for examining expression of TEs in

488 young and old w^{1118}. RNA was DNase treated (Invitrogen) and cDNA was synthesized

489 using the Verso cDNA kit (Thermo-Fisher AB1453A). 1-5μg of RNA was used for cDNA

490 creation. PowerUp SYBR Green Master Mix was used to perform qPCR on the Applied

491 Biosystems QuantStudio3 system. *rp49* (*RpL32*) was used as the housekeeping gene

492 to normalize relative gene expression changes. Experiments were performed in 3-5

493 biological replicates. An unpaired t-test with Bonferroni correction was used as the

494 statistical test. Primers used in these experiments can be found in the S9 Table. (11,

495 75-82)

496

497 **Lifespan quantification**

498 Adult flies were collected 48 hours after eclosion and mated for 24 hours. Flies were

499 sorted by sex and genotype and placed at a density of no more than 25 flies per vial.

500 The number of dead animals was counted twice a week and remaining live flies were

501 transferred to new food vials. Lifespan experiments were performed in triplicate

502 (separate crosses) and results pooled. A Dunnett test was used to compare survival

503 curves. A Gehan-Breslow-Wilcoxon test was used to compare median lifespan.

504   Difference in maximum lifespan was calculated by a permutation test (95th percentile)

505   followed by two-sided t-test with correction for multiple comparisons.

506

507   **Oxidative stress survival**

508   Flies were placed on 20mM paraquat (Sigma), 1% agar, 5% sucrose media at day 40

509   post eclosion. The number of dead animals were counted every 4-8 hours until all flies

510   were dead. The experiment was performed in biological triplicate. A Dunnett test was

511   used to compare survival curves.

512

513   **Starvation survival**

514   Day 40 adult flies were provided with Whatman paper-soaked in water and the number

515   of dead animals counted every 4 hours until all flies were dead. The experiment was

516   performed in biological triplicate. A Dunnett test was used to compare survival curves.

517

518   **Endoplasmic reticulum stress survival**

519   Flies were placed on 12 μM tunicamycin (Sigma), 1.5% agar, and 5% sucrose media at

520   day 20 post eclosion. The number of dead animals were counted every day until all flies

521   were dead. The experiment was performed in biological triplicate. A Dunnett test was

522   used to compare survival curves.

523

524   **Negative geotaxis**

525   Flies at days 5, 20, and 40 post eclosion were recorded while they were tapped down to

526   the bottom of empty vials. After 10 seconds the number of flies in each third of each vial

527   were counted. Flies were allowed a minute to recover before the experiment was

528   repeated. The experiment was performed a total of three times in biological triplicate. A

529   Chi-square test for trend was used to compare the locomotor activity of the different

530   genotypes.

531

Fecundity and Fertility

533   Females were mated with w^{1118} males (1:1 ratio) at day 25 post eclosion at a density of

534   approximately 20 flies per vial. Females were given 24 hours to lay eggs, then

535   transferred to a new vial and the eggs per vial were counted every day for 5 days.

536   Fecundity was calculated as the average number of eggs laid per vial per day. To

537   assess fertility, the number of eggs laid was quantified and animals allowed to develop

538   until eclosion at which point the number of adults flies were quantified. The fertility index

539   was calculated by dividing the number of adult flies by the number of eggs laid per vial.

540   A fertility index of 1 is defined as 100% fertile. A One-way ANOVA was used to

541   calculate the differences in fecundity and fertility across genotypes.

542

Thermal stress survival

544   To test sensitivity to cold stress, flies were placed in new food vials and placed at 4℃ on

545   ice for 15 hours at day 20 post eclosion. Flies were given 48 hours to recover at 25℃

546   and the number dead flies counted. To test heat sensitivity, flies were placed in new

547   food vials and placed at 37℃ until about 80% of flies were immobile at the bottom of the

548   vial with heat paralysis. Flies were given 48 hours to recover at 25℃ and the number of

24

549   dead flies were counted. Assays were performed in biological triplicate. A Fisher's exact

550   test was used to calculate the difference in survival across genotypes.

551

552   **Body weight and animal size**

553   Zeiss Discovery.V12 SteREO with the AxioVision Release 4.8 software was used to

554   capture pictures of adult flies using a ruler to show size. All images were processed

555   using Adobe Photoshop. Flies were 2 days post eclosion for imaging and body mass

556   quantification. To measure body mass, 10 flies of each genotype were placed in 1.5mL

557   Eppendorf tube and weighed. This was done in biological triplicate. A One-way ANOVA

558   was used to calculate body weight differences across genotypes.

559

560   **Purification and amplification of individual thoracic nuclei**

561   40-60 thoraces from young (5 days old) or old (50 days old) w^{1118} flies were dissected

562   and single nuclei were prepared according to (83) with minor alterations. Briefly, instead

563   of using a Polytron, thoraces were homogenized with an automatic pestle for 5 minutes

564   on ice, transferred to a 7mL Dounce homogenizer and pulverized with 30 stokes of the

565   pestle. Debris was filtered using a 20-micron filter and subsequently with a 10-micron

566   filter (twice). Nuclei were then sorted into individual tubes using the CellRaft AIR®

567   System. Genomic DNA from each nucleus was amplified by multiple displacement

568   amplification and made into libraries according to (84). Libraries (21 per group) were

569   subjected to paired end whole genome sequencing (WGS) on the Illumina 2500

570   platform at Novogene. The data discussed in this publication have been deposited in

571   NCBI's Sequence Read Archive and are accessible through BioProject accession

572   number: PRJNA854389.

573

Purification and genome amplification of IFM nuclei

575   UH3-Gal4/ +; +/+; UAS-Klar-KASH/+ flies were aged to either 5 (young) or 60 (old)

576   days. 50 thoraces per group were dissected and single nuclei were prepared using the

577   nuclei EZ isolation kit (Sigma) according to manufacturer instructions. Nuclei were then

578   stained with DAPI, and fluorescence-activated cell sorting (FACS) sorted gaiting for

579   DAPI (4′,6-diamidino-2-phenylindole) and GFP positive populations using the

580   MoFloXDP at the Flow Cytometry Core Facility at Albert Einstein College of Medicine.

581   The first gate selected for size by plotting forward scatter (FSC, size) against side

582   scatter (SSC, granularity), with debris being outside the gate. 99.6% of the population

583   was not debris. A log scale was used to visualize high signals from both axes in the

584   same plot. The second gate selected for single nuclei by plotting SSC-width (doublets)

585   against SSC-height (intensity). Single nuclei were 30.14% of the population. The last

586   and final gate selected for intact IFM nuclei by plotting GFP (IFM) against DAPI (DNA).

587   The nuclei were sorted into individual tubes and subject to single nucleus whole

588   genome amplification (snWGA) using the REPLI-g® UltraFast Mini kit (Qiagen). The

589   snWGA was performed by a multiple displacement amplification as in this previous

590   publication (85). The snWGA amplicons were purified using AMPure XP magnetic

591   beads (Agencourt). The snWGA amplicons were then subject to a locus drop out (LDO)

592   test to screen for amplification of five regions dispersed throughout the genome, similar

593   to previous studies (86). The Fast SYBR® Green Master Mix (Applied Biosystems) was

26

594   used for the qPCR reaction. Nuclei with the most primer sets passing the LDO test were

595   subjected to paired end sequencing (scWGS) on the Illumina 2500 platform at

596   Novogene. Bulk/pooled unamplified genomic DNA from young abdominal segments

597   was used as the control for genomic insertions already present in the strain. The data

598   discussed in this publication have been deposited in NCBI's Sequence Read Archive

599   and are accessible through BioProject accession number: PRJNA854818.

600

601   **Bioinformatic analyses of single nucleus data**

602   To control for genetic background germline TE insertions, genomic DNA was extracted

603   from pooled young (day 5) thoraces from 50 flies and sequenced at Novogene. Fastq

604   files were analyzed using the new pipeline Retrofind and also the published pipeline

605   from the Bardin lab (27). Retrofind pre-filters input sequencing reads to require at least

606   one mate pair to contain retrotransposon DNA sequences. Next, Retrofind conducts an

607   alignment on the pre-filtered reads using the BWA mem aligner under strict conditions

608   (87). Samtools coordinate sorts and Picard tools removes duplicates from the alignment

609   (88). Reads inconsistent with a proper mate pairing or with larger than expected insert

610   size are identified as a discordant read pair. Split reads are identified from reads

611   aligning with soft or hard clipping above a threshold. Candidate split and discordant

612   reads are aligned using BWA mem to a list of consensus sequences derived from

613   Repbase (89). Candidate reads are then grouped into clusters using bedtools and

614   designated as 5' (left) and 3' (right) junction reads (90). Next, a heuristic process is

615   applied to the left and right junction to identify a retrotransposition that satisfies filtering

616   options. If there is at least one right junction and one left junction split read, a target site

27

617   duplication (TSD) prediction is made. There is an option to require a TSD prediction

618   within a user-defined range. The default TSD size range we consider is 2-30 base pairs.

619   The exported file includes an identification number that can be used to link reads of

620   support to the transposition call. Lastly, Retrofind also outputs *de novo* assembly of

621   supporting reads using the Megahit short read assembler (91) and a BWA mem

622   alignment of assembled contigs to the genome. The reads of support and assembled

623   contig alignment can be visually inspected using a genome browser. Retrofind was

624   validated using the pipeline and methods described in (27).

625   *De novo* TE insertions detected in both young and old IFM nuclei compared to

626   the bulk genomic DNA to exclude the insertions that are present within the germline.

627   The genomic location of insertions identified in w^{1118} were determined using

628   ChIPSeeker (92). High quality insertions were defined as insertions detected within both

629   pipelines and validated in IGV.

630

631   **Data Accessibility**

632   RNA-seq data can be accessed through GEO Series accession number GSE207160.

633   The thoracic WGS data can be accessed through the Sequence Read Archive (SRA)

634   and are accessible through BioProject accession number: PRJNA854389. The indirect

635   flight muscle WGS data can be accessed through the SRA BioProject accession

636   number: PRJNA854818.

637

638   **Acknowledgements**

648

649   **Supporting information captions**

650   **Fig 1. Single cell whole genome sequencing of young (day 5) and old (day 50)**

651   ***Drosophila* thoraces**

652   (A) A schematic of the workflow of the isolation of single nuclei and how new TE

653   insertions were detected. The typical w^{1118} wild type strain lifespan is also displayed.

654   (B)The number of new TE insertions in the w^{1118} strain from the bulk WGS in

655   comparison to the sequenced reference strain (dm6) using both the pipeline from

656   Siudeja et al (27) and Retrofind. 505 insertions were called by both pipelines. (C) The

657   distribution of the genomic locations where the w^{1118} strain TE insertions fall. (D) The

658   number of known TE insertions (strain/background insertions) that were able to be

659   detected within each nuclear sample represented as a percentage of the insertions

660   detected in the sample out of total strain insertions. Each dot represents a nucleus. (E)

661   The number of new TE insertions within each nucleus that are not previously called

662 within the strain or other nuclei. Each dot represents a nucleus. Unpaired t-test. ns p=

663 0.1809. (F) The distribution of genomic locations where the 15 new TE insertions within

664 individual nuclei fall. (G) qPCR using SYBR green showing levels of TE mRNA relative

665 to Rp49 (Rpl32) from adult w^{1118} flies young (day 5) in blue and old (day 50) in red head

666 and thoraces. The experiment was performed in three biological replicates. An unpaired

667 t-test with Bonferroni correction was used. *** (*Accord*) p= 0.0009 ** (*Blastopia*) p=

668 0.0020. * (*Blood*) p= 0.0262. *** (*Copia*) p= 0.0007. * (*gypsy12*) p= 0.0171. ** (*HMS-*

669 *Beagle*) p= 0.0011. ** (*Tahre*) p= 0.0038. ** (*Springer*) p= 0.0026. ns (*412*) p= 0.1453.

670 ns (*Bari2*) p=0.7403. ns (*DM1731*) p= 0.0702. ns (*McClintock*) p= 0.1814. ns (*Roo*) p=

671 0.7985. ns (*Stalker4*) p= 0.7957. ** (*297*) p= 0.0012. *** (*Tabor*) p= 0.0005.

672

673 **Fig 2. Single cell whole genome sequencing of young (day 5) and old (day 60)**

674 ***Drosophila* indirect flight muscles**

675 (A) A schematic of the workflow of the isolation of single nuclei and how new TE

676 insertions were detected from indirect flight muscles (IFMs). (B) The number of new TE

677 insertions within each nucleus that are not previously called within the strain or other

678 nuclei. Each dot represents a nucleus. Unpaired t-test. ns p >0.9999. (C) The

679 distribution of genomic locations where the new TE insertions within individual nuclei

680 fall.

681

682 **Fig 3. Lifespan of ubiquitous shRNA and CRISPRi knockdown of the**

683 **retrotransposons, *412* and *Roo***

684   (A) qPCR using SYBR green showing levels of *412* mRNA relative to *Rp49* (*Rpl32*) from

685   adult flies expressing a control shRNA transgene under the control of Act5C-Gal4

686   compared to the *412* shRNA knockdowns (Act5C>shRNA). The experiment was

687   performed in five biological replicates. An unpaired t-test with Bonferroni correction was

688   used. ** p=0.0018. * p=0.0219. (B) Survival of the *412* shRNA lines compared to control

689   shRNA driven ubiquitously by Act5C (Act>shRNA). Dunnett test. ****p <0.0001. (C)

690   Median lifespan of the *412* shRNAs compared to control shRNA driven ubiquitously by

691   Act5C (Act>shRNA). Gehan-Breslow-Wilcoxon test. ****p<0.0001. (D) Maximum

692   lifespan of the *412* shRNAs compared to control shRNA driven ubiquitously by Act5C

693   (Act>shRNA). Permutation test (95th percentile/top 5%) followed by two-sided t-test with

694   correction for multiple comparisons. ****p<0.0001. ***p= 0.0001. (E) qPCR using SYBR

695   green of 412gRNA CRISPRi compared to the control gRNA control (Act5C>dcas9-

696   KRAB) relative to *Rp49* (*Rpl32*). An unpaired t-test with Bonferroni correction was used.

697   * p=0.0269. (F) Survival of the CRISPRi driven ubiquitously by Act5C (Act>dcas9KRAB)

698   with the 412gRNA compared to control gRNA. Dunnett test. **** p <0.0001. (G) Median

699   lifespan of the CRISPRi driven ubiquitously by Act5C (Act>dcas9KRAB) with the

700   412gRNA compared to control gRNA. Gehan-Breslow-Wilcoxon test. **** p <0.0001. (H)

701   Maximum lifespan of the of the CRISPRi driven ubiquitously by Act5C

702   (Act>dcas9KRAB) with the 412gRNA compared to control gRNA. Permutation test (95th

703   percentile) followed by two-sided t-test with correction for multiple comparisons. *

704   p=0.0377. (I) qPCR using SYBR green of the *Roo* mRNA KD compared to the control

705   shRNA control (Act5C>shRNA) relative to *Rp49* (*Rpl32*). The experiment was

706   performed in six biological replicates. An unpaired t-test with Bonferroni correction was

707   used. ** p=0.0022. (J) Survival of the *Roo* shRNA compared to control shRNA driven

708   ubiquitously by Act5C (Act>shRNA). Dunnett test. **** p <0.0001 (K) Median lifespan of

709   the *Roo* shRNA compared to control shRNA driven ubiquitously by Act5C (Act>shRNA).

710   Gehan-Breslow-Wilcoxon test. **** p <0.0001. (L) Maximum lifespan of the *Roo* shRNA

711   compared to control shRNA driven ubiquitously by Act5C (Act>shRNA). Permutation

712   test (95th percentile) followed by two-sided t-test with correction for multiple

713   comparisons. **** p<0.0001.

714

715   **Fig 4. Stress resistance assays of *412* and *Roo* knockdown animals**

716   (A) Act5c>shRNA day 18 measurement of locomotion via negative geotaxis assay. The

717   percentages of flies in each third of the vial is displayed. Chi-square test for trend. *

718   (412#1) p=0.0428. ns (412#2) p=0.1434. ns (Roo) p=0.1934. (B) Act5c>shRNA day 40

719   response to oxidative stress by feeding paraquat and measuring survival. Dunnett test.

720   **** (412#1) p<0.0001. ns (412#2) p= 0.0702. ns (Roo) p >0.9999. (C) Act5c>shRNA

721   day 20 response to endoplasmic reticulum (ER) stress by feeding tunicamycin and

722   measuring survival. Dunnett test. ns (412#1) p=0.0826. ** (412#2) p=0.0046. ns (Roo)

723   p=0.1721. (D) Act5c>shRNA day 40 response to starvation by only giving the flies

724   access to water and measuring survival. Dunnett test. ns (412#1) p=0.8332. ns (412#2)

725   p=0.5694. ns (Roo) p=0.2239. (E) Act5c>shRNA day 20 response to cold stress by

726   keeping flies at 4 degrees Celsius and measuring survival after 48-hours recovery. Each

727   dot is a vial or replicate of approximately 20 flies. Fisher's exact test. ns (412#1)

728   p=0.0703. * (412#2) p= 0.0461. ns (Roo) p= 0.6592. (F) Act5c>shRNA day 20 response

729   to heat stress by keeping flies at 37 degrees Celsius and measuring survival after 48-

730   hours recovery. Each dot is a replicate of approximately 20 flies. Fisher's exact test. ns

731   (412#1) p= 0.0915. ns (412#2) p= 0.7643. ns (Roo) p= 0.5061. (G) Act5c>shRNA day

732   25 measurement of fecundity. Data is displayed as average number of eggs laid per day

733   over 5 days. Each dot represents a day for the number of flies in one vial. One-way

734   ANOVA. ns (412#1) p=0.9925. ns (412#2) p=0.7231. ns (Roo) p=0.1803. (H)

735   Act5c>shRNA day 25 measurement of fertility. Fertility index is calculated as number of

736   progeny divided by number of eggs laid. Data is displayed as average fertility index over

737   5 days. Each dot represents a day for the number of flies listed. One-way ANOVA. ns

738   (412#1) p>0.9999. ns (412#2) p=0.5881. ns (Roo) p=0.9887.

739

740   **Fig 5. Transcriptomic analysis of *412* and *Roo* knockdown animals**

741   (A) Volcano plot of differentially expressed genes (DEGs) from whole thorax of

742   Act5c>412#1 shRNA knockdown animals compared to control shRNA animals. Genes

743   with a false discovery rate (FDR) <0.05 are highlighted in black and above the dashed

744   line. Genes that are differentially expressed in both *412* and *Roo* knockdown animals

745   (overlapping genes) are highlighted in red. (B) Volcano plot of differentially expressed

746   genes (DEGs) from whole thorax of Act5c>Roo shRNA knockdown animals compared

747   to control shRNA animals. Genes with a false discovery rate (FDR) <0.05 are

748   highlighted in black and above the dashed line. Genes that are differentially expressed

749   in both *412* and *Roo* knockdown animals (overlapping genes) are highlighted in red. (C)

750   Correlation of Log$_2$FoldChange (Log2FC) of the overlapping DEGs between *412* and

751   *Roo* knockdown animals. r=0.9461. Deming regression. p<0.0001. Serine proteases

752   and AMPs that are also DEGS are enlarged and highlighted in purple. (D) Protein

33

753   clustering performed on the overlapping DEGs using String with single nodes removed

754   and 1 cluster used. There is a serine protease cluster of genes interacting. (E) Heatmap

755   of log2fold change (Log2FC) from RNA-seq data across samples of the *Jonah* (*Jon*)

756   genes. The * marked genes are significantly differentially expressed in both *412* and

757   *Roo* knockdown thoraces. All other genes are significantly differentially expressed in

758   just *412* knockdown thoraces. (F) Heatmap of log2fold change (Log2FC) across

759   samples of the antimicrobial peptides (AMPs). The * marked genes are significantly

760   differentially expressed in both *412* and *Roo* knockdown thoraces. All other genes are

761   significantly differentially expressed in just *412* knockdown thoraces.

762

REFERENCES

764   1.   Health, United States, 2019, (2021).
765   2.   Dong X, Milholland B, Vijg J. Evidence for a limit to human lifespan. Nature.
766   2016;538(7624):257-9.
767   3.   Vijg J, Suh Y. Genome instability and aging. Annu Rev Physiol. 2013;75:645-68.
768   4.   López-Otín C, Blasco MA, Partridge L, Serrano M, Kroemer G. The hallmarks of aging.
769   Cell. 2013;153(6):1194-217.
770   5.   Lander ES, Linton LM, Birren B, Nusbaum C, Zody MC, Baldwin J, et al. Initial sequencing
771   and analysis of the human genome. Nature. 2001;409(6822):860-921.
772   6.   Miao B, Fu S, Lyu C, Gontarz P, Wang T, Zhang B. Tissue-specific usage of transposable
773   element-derived promoters in mouse development. Genome Biol. 2020;21(1):255.
774   7.   Hoskins RA, Smith CD, Carlson JW, Carvalho AB, Halpern A, Kaminker JS, et al.
775   Heterochromatic sequences in a Drosophila whole-genome shotgun assembly. Genome Biol.
776   2002;3(12):Research0085.
777   8.   McCullers TJ, Steiniger M. Transposable elements in Drosophila. Mob Genet Elements.
778   2017;7(3):1-18.
779   9.   Smith CD, Shu S, Mungall CJ, Karpen GH. The Release 5.1 annotation of Drosophila
780   melanogaster heterochromatin. Science. 2007;316(5831):1586-91.
781   10.   De Cecco M, Criscione SW, Peckham EJ, Hillenmeyer S, Hamm EA, Manivannan J, et al.
782   Genomes of replicatively senescent cells undergo global epigenetic changes leading to gene
783   silencing and activation of transposable elements. Aging Cell. 2013;12(2):247-56.

784   11.   Chen H, Zheng X, Xiao D, Zheng Y. Age-associated de-repression of retrotransposons in
785   the Drosophila fat body, its potential cause and consequence. Aging Cell. 2016;15(3):542-52.
786   12.   Pray LA. Transposons: The Jumping Genes. Nature Education. 2008;1(1)(204).
787   13.   Levin HL, Moran JV. Dynamic interactions between transposable elements and their
788   hosts. Nat Rev Genet. 2011;12(9):615-27.
789   14.   Simon M, Van Meter M, Ablaeva J, Ke Z, Gonzalez RS, Taguchi T, et al. LINE1
790   Derepression in Aged Wild-Type and SIRT6-Deficient Mice Drives Inflammation. Cell Metab.
791   2019;29(4):871-85.e5.
792   15.   De Cecco M, Ito T, Petrashen AP, Elias AE, Skvir NJ, Criscione SW, et al. L1 drives IFN in
793   senescent cells and promotes age-associated inflammation. Nature. 2019;566(7742):73-8.
794   16.   Miller KN, Victorelli SG, Salmonowicz H, Dasgupta N, Liu T, Passos JF, et al. Cytoplasmic
795   DNA: sources, sensing, and role in aging and disease. Cell. 2021;184(22):5506-26.
796   17.   Janssen A, Colmenares SU, Karpen GH. Heterochromatin: Guardian of the Genome.
797   Annu Rev Cell Dev Biol. 2018;34:265-88.
798   18.   Gorbunova V, Seluanov A, Mita P, McKerrow W, Fenyö D, Boeke JD, et al. The role of
799   retrotransposable elements in ageing and age-associated diseases. Nature. 2021;596(7870):43-
800   53.
801   19.   Gorbunova V, Boeke JD, Helfand SL, Sedivy JM. Human Genomics. Sleeping dogs of the
802   genome. Science. 2014;346(6214):1187-8.
803   20.   Li W, Prazak L, Chatterjee N, Grüninger S, Krug L, Theodorou D, et al. Activation of
804   transposable elements during aging and neuronal decline in Drosophila. Nat Neurosci.
805   2013;16(5):529-31.
806   21.   Sioud M. RNA Interference: Story and Mechanisms. Methods Mol Biol. 2021;2282:1-15.
807   22.   Wang JH, Valanne S, Rämet M. Drosophila as a model for antiviral immunity. World J
808   Biol Chem. 2010;1(5):151-9.
809   23.   Wood JG, Jones BC, Jiang N, Chang C, Hosier S, Wickremesinghe P, et al. Chromatin-
810   modifying genetic interventions suppress age-associated transposable element activation and
811   extend life span in Drosophila. Proc Natl Acad Sci U S A. 2016;113(40):11277-82.
812   24.   Yang N, Srivastav SP, Rahman R, Ma Q, Dayama G, Li S, et al. Transposable element
813   landscapes in aging Drosophila. PLoS Genet. 2022;18(3):e1010024.
814   25.   Driver CJ, Vogrig DJ. Apparent retardation of aging in Drosophila melanogaster by
815   inhibitors of reverse transcriptase. Ann N Y Acad Sci. 1994;717:189-97.
816   26.   Chang YH, Keegan RM, Prazak L, Dubnau J. Cellular labeling of endogenous retrovirus
817   replication (CLEVR) reveals de novo insertions of the gypsy retrotransposable element in cell
818   culture and in both neurons and glial cells of aging fruit flies. PLoS Biol. 2019;17(5):e3000278.
819   27.   Siudeja K, van den Beek M, Riddiford N, Boumard B, Wurmser A, Stefanutti M, et al.
820   Unraveling the features of somatic transposition in the Drosophila intestine. Embo j.
821   2021;40(9):e106388.
822   28.   Qiu S, Xiao C, Meldrum Robertson R. Different age-dependent performance in
823   Drosophila wild-type Canton-S and the white mutant w1118 flies. Comp Biochem Physiol A Mol
824   Integr Physiol. 2017;206:17-23.
825   29.   Periquet G, Lemeunier F, Bigot Y, Hamelin MH, Bazin C, Ladevèze V, et al. The
826   evolutionary genetics of the hobo transposable element in the Drosophila melanogaster
827   complex. Genetica. 1994;93(1-3):79-90.

828 30.   Josephson RK, Malamud JG, Stokes DR. Asynchronous muscle: a primer. J Exp Biol.
829 2000;203(Pt 18):2713-22.
830 31.   Agianian B, Krzic U, Qiu F, Linke WA, Leonard K, Bullard B. A troponin switch that
831 regulates muscle contraction by stretch instead of calcium. Embo j. 2004;23(4):772-9.
832 32.   Jawkar S, Nongthomba U. Indirect flight muscles in Drosophila melanogaster as a
833 tractable model to study muscle development and disease. Int J Dev Biol. 2020;64(1-2-3):167-
834 73.
835 33.   Demontis F, Patel VK, Swindell WR, Perrimon N. Intertissue control of the nucleolus via a
836 myokine-dependent longevity pathway. Cell Rep. 2014;7(5):1481-94.
837 34.   Singh SH, Kumar P, Ramachandra NB, Nongthomba U. Roles of the troponin isoforms
838 during indirect flight muscle development in Drosophila. J Genet. 2014;93(2):379-88.
839 35.   Di Franco C, Galuppi D, Junakovic N. Genomic distribution of transposable elements
840 among individuals of an inbred Drosophila line. Genetica. 1992;86(1-3):1-11.
841 36.   Gramates LS, Agapite J, Attrill H, Calvi BR, Crosby MA, Dos Santos G, et al. Fly Base: a
842 guided tour of highlighted features. Genetics. 2022;220(4).
843 37.   Broughton SJ, Piper MD, Ikeya T, Bass TM, Jacobson J, Driege Y, et al. Longer lifespan,
844 altered metabolism, and stress resistance in Drosophila from ablation of cells making insulin-
845 like ligands. Proc Natl Acad Sci U S A. 2005;102(8):3105-10.
846 38.   Cassidy D, Epiney DG, Salameh C, Zhou LT, Salomon RN, Schirmer AE, et al. Evidence for
847 premature aging in a Drosophila model of Werner syndrome. Exp Gerontol. 2019;127:110733.
848 39.   Sun Y, Yolitz J, Wang C, Spangler E, Zhan M, Zou S. Aging studies in Drosophila
849 melanogaster. Methods Mol Biol. 2013;1048:77-93.
850 40.   Chow CY, Wolfner MF, Clark AG. Using natural variation in Drosophila to discover
851 previously unknown endoplasmic reticulum stress genes. Proc Natl Acad Sci U S A.
852 2013;110(22):9013-8.
853 41.   Jasienska G, Nenko I, Jasienski M. Daughters increase longevity of fathers, but daughters
854 and sons equally reduce longevity of mothers. Am J Hum Biol. 2006;18(3):422-5.
855 42.   Huang da W, Sherman BT, Lempicki RA. Systematic and integrative analysis of large gene
856 lists using DAVID bioinformatics resources. Nat Protoc. 2009;4(1):44-57.
857 43.   Sherman BT, Hao M, Qiu J, Jiao X, Baseler MW, Lane HC, et al. DAVID: a web server for
858 functional enrichment analysis and functional annotation of gene lists (2021 update). Nucleic
859 Acids Res. 2022;50(W1):W216-21.
860 44.   Szklarczyk D, Gable AL, Nastou KC, Lyon D, Kirsch R, Pyysalo S, et al. The STRING
861 database in 2021: customizable protein-protein networks, and functional characterization of
862 user-uploaded gene/measurement sets. Nucleic Acids Res. 2021;49(D1):D605-d12.
863 45.   Miguel-Aliaga I, Jasper H, Lemaitre B. Anatomy and Physiology of the Digestive Tract of
864 Drosophila melanogaster. Genetics. 2018;210(2):357-96.
865 46.   Akam ME, Carlson JR. The detection of Jonah gene transcripts in Drosophila by in situ
866 hybridization. Embo j. 1985;4(1):155-61.
867 47.   Yadav S, Eleftherianos I. Participation of the Serine Protease Jonah66Ci in the Drosophila
868 Antinematode Immune Response. Infect Immun. 2019;87(9).
869 48.   Carpenter J, Hutter S, Baines JF, Roller J, Saminadin-Peter SS, Parsch J, et al. The
870 transcriptional response of Drosophila melanogaster to infection with the sigma virus
871 (Rhabdoviridae). PLoS One. 2009;4(8):e6838.

872 49.   Ward JR, Khan A, Torres S, Crawford B, Nock S, Frisbie T, et al. Condensin I and
873 condensin II proteins form a LINE-1 dependent super condensin complex and cooperate to
874 repress LINE-1. Nucleic Acids Res. 2022.
875 50.   Rigal J, Martin Anduaga A, Bitman E, Rivellese E, Kadener S, Marr MT. Artificially
876 stimulating retrotransposon activity increases mortality and accelerates a subset of aging
877 phenotypes in Drosophila. Elife. 2022;11.
878 51.   Scott EC, Gardner EJ, Masood A, Chuang NT, Vertino PM, Devine SE. A hot L1
879 retrotransposon evades somatic repression and initiates human colorectal cancer. Genome Res.
880 2016;26(6):745-55.
881 52.   Cajuso T, Sulo P, Tanskanen T, Katainen R, Taira A, Hänninen UA, et al. Retrotransposon
882 insertions can initiate colorectal cancer and are associated with poor survival. Nat Commun.
883 2019;10(1):4022.
884 53.   Hancks DC, Kazazian HH, Jr. Roles for retrotransposon insertions in human disease. Mob
885 DNA. 2016;7:9.
886 54.   Martin M, Hiroyasu A, Guzman RM, Roberts SA, Goodman AG. Analysis of Drosophila
887 STING Reveals an Evolutionarily Conserved Antimicrobial Function. Cell Rep. 2018;23(12):3537-
888 50.e6.
889 55.   Khor S, Cai D. Control of lifespan and survival by Drosophila NF-κB signaling through
890 neuroendocrine cells and neuroblasts. Aging (Albany NY). 2020;12(24):24604-22.
891 56.   Valanne S, Wang JH, Rämet M. The Drosophila Toll signaling pathway. J Immunol.
892 2011;186(2):649-56.
893 57.   Myllymäki H, Valanne S, Rämet M. The Drosophila imd signaling pathway. J Immunol.
894 2014;192(8):3455-62.
895 58.   Lin YR, Parikh H, Park Y. Stress resistance and lifespan enhanced by downregulation of
896 antimicrobial peptide genes in the Imd pathway. Aging (Albany NY). 2018;10(4):622-31.
897 59.   Hu Y, Flockhart I, Vinayagam A, Bergwitz C, Berger B, Perrimon N, et al. An integrative
898 approach to ortholog prediction for disease-focused and other functional studies. BMC
899 Bioinformatics. 2011;12:357.
900 60.   Hu Y, Comjean A, Roesel C, Vinayagam A, Flockhart I, Zirin J, et al. FlyRNAi.org-the
901 database of the Drosophila RNAi screening center and transgenic RNAi project: 2017 update.
902 Nucleic Acids Res. 2017;45(D1):D672-d8.
903 61.   Hu Y, Comjean A, Rodiger J, Liu Y, Gao Y, Chung V, et al. FlyRNAi.org—the database of
904 the Drosophila RNAi screening center and transgenic RNAi project: 2021 update. Nucleic Acids
905 Research. 2020;49(D1):D908-D15.
906 62.   Parekh VJ, Rathod VK, Pandit AB. 2.10 - Substrate Hydrolysis: Methods, Mechanism, and
907 Industrial Applications of Substrate Hydrolysis. In: Moo-Young M, editor. Comprehensive
908 Biotechnology (Second Edition). Burlington: Academic Press; 2011. p. 103-18.
909 63.   Shah D, Mital K. The Role of Trypsin:Chymotrypsin in Tissue Repair. Adv Ther.
910 2018;35(1):31-42.
911 64.   Perkins LA, Holderbaum L, Tao R, Hu Y, Sopko R, McCall K, et al. The Transgenic RNAi
912 Project at Harvard Medical School: Resources and Validation. Genetics. 2015;201(3):843-52.
913 65.   Foveau N. DSIR Designer of small interfering RNA Cartes d'Identite des Tumeurs"
914 program (CIT): Ligue Nationale Contre le Cancer; 2007 [

915   66.   Port F, Bullock SL. Augmenting CRISPR applications in Drosophila with tRNA-flanked
916   sgRNAs. Nat Methods. 2016;13(10):852-4.
917   67.   Port F, Chen HM, Lee T, Bullock SL. Optimized CRISPR/Cas tools for efficient germline
918   and somatic genome engineering in Drosophila. Proc Natl Acad Sci U S A. 2014;111(29):E2967-
919   76.
920   68.   Port F, Muschalik N, Bullock SL. Systematic Evaluation of Drosophila CRISPR Tools
921   Reveals Safe and Robust Alternatives to Autonomous Gene Drives in Basic Research. G3
922   (Bethesda). 2015;5(7):1493-502.
923   69.   Port F, Starostecka M, Boutros M. Multiplexed conditional genome editing with Cas12a
924   in Drosophila. Proc Natl Acad Sci U S A. 2020;117(37):22890-9.
925   70.   Port F, Strein C, Stricker M, Rauscher B, Heigwer F, Zhou J, et al. A large-scale resource
926   for tissue-specific CRISPR mutagenesis in Drosophila. Elife. 2020;9.
927   71.   Heigwer F, Port F, Boutros M. RNA Interference (RNAi) Screening in Drosophila.
928   Genetics. 2018;208(3):853-74.
929   72.   Akbari OS, Bellen HJ, Bier E, Bullock SL, Burt A, Church GM, et al. BIOSAFETY.
930   Safeguarding gene drive experiments in the laboratory. Science. 2015;349(6251):927-9.
931   73.   Kim D, Paggi JM, Park C, Bennett C, Salzberg SL. Graph-based genome alignment and
932   genotyping with HISAT2 and HISAT-genotype. Nat Biotechnol. 2019;37(8):907-15.
933   74.   Edgar R, Domrachev M, Lash AE. Gene Expression Omnibus: NCBI gene expression and
934   hybridization array data repository. Nucleic Acids Res. 2002;30(1):207-10.
935   75.   Ghildiyal M, Seitz H, Horwich MD, Li C, Du T, Lee S, et al. Endogenous siRNAs derived
936   from transposons and mRNAs in Drosophila somatic cells. Science. 2008;320(5879):1077-81.
937   76.   Klein JD, Qu C, Yang X, Fan Y, Tang C, Peng JC. c-Fos Repression by Piwi Regulates
938   Drosophila Ovarian Germline Formation and Tissue Morphogenesis. PLoS Genet.
939   2016;12(9):e1006281.
940   77.   Matsumoto N, Sato K, Nishimasu H, Namba Y, Miyakubi K, Dohmae N, et al. Crystal
941   Structure and Activity of the Endoribonuclease Domain of the piRNA Pathway Factor
942   Maelstrom. Cell Rep. 2015;11(3):366-75.
943   78.   Kalmykova AI, Klenov MS, Gvozdev VA. Argonaute protein PIWI controls mobilization of
944   retrotransposons in the Drosophila male germline. Nucleic Acids Res. 2005;33(6):2052-9.
945   79.   Hur JK, Luo Y, Moon S, Ninova M, Marinov GK, Chung YD, et al. Splicing-independent
946   loading of TREX on nascent RNA is required for efficient expression of dual-strand piRNA
947   clusters in Drosophila. Genes Dev. 2016;30(7):840-55.
948   80.   Drelon C, Rogers MF, Belalcazar HM, Secombe J. The histone demethylase KDM5
949   controls developmental timing in Drosophila by promoting prothoracic gland endocycles.
950   Development. 2019;146(24).
951   81.   Dufourt J, Dennis C, Boivin A, Gueguen N, Théron E, Goriaux C, et al. Spatio-temporal
952   requirements for transposable element piRNA-mediated silencing during Drosophila oogenesis.
953   Nucleic Acids Res. 2014;42(4):2512-24.
954   82.   Czech B, Malone CD, Zhou R, Stark A, Schlingeheyde C, Dus M, et al. An endogenous
955   small interfering RNA pathway in Drosophila. Nature. 2008;453(7196):798-802.
956   83.   Corces MR, Trevino AE, Hamilton EG, Greenside PG, Sinnott-Armstrong NA, Vesuna S, et
957   al. An improved ATAC-seq protocol reduces background and enables interrogation of frozen
958   tissues. Nat Methods. 2017;14(10):959-62.

959   84.   Dong X, Zhang L, Milholland B, Lee M, Maslov AY, Wang T, et al. Accurate identification
960   of single-nucleotide variants in whole-genome-amplified single cells. Nat Methods.
961   2017;14(5):491-3.
962   85.   Dean FB, Hosono S, Fang L, Wu X, Faruqi AF, Bray-Ward P, et al. Comprehensive human
963   genome amplification using multiple displacement amplification. Proc Natl Acad Sci U S A.
964   2002;99(8):5261-6.
965   86.   Gundry M, Li W, Maqbool SB, Vijg J. Direct, genome-wide assessment of DNA mutations
966   in single cells. Nucleic Acids Res. 2012;40(5):2032-40.
967   87.   Li H, Durbin R. Fast and accurate short read alignment with Burrows-Wheeler transform.
968   Bioinformatics. 2009;25(14):1754-60.
969   88.   Li H, Handsaker B, Wysoker A, Fennell T, Ruan J, Homer N, et al. The Sequence
970   Alignment/Map format and SAMtools. Bioinformatics. 2009;25(16):2078-9.
971   89.   Bao W, Kojima KK, Kohany O. Repbase Update, a database of repetitive elements in
972   eukaryotic genomes. Mob DNA. 2015;6:11.
973   90.   Quinlan AR, Hall IM. BEDTools: a flexible suite of utilities for comparing genomic
974   features. Bioinformatics. 2010;26(6):841-2.
975   91.   Li D, Liu CM, Luo R, Sadakane K, Lam TW. MEGAHIT: an ultra-fast single-node solution
976   for large and complex metagenomics assembly via succinct de Bruijn graph. Bioinformatics.
977   2015;31(10):1674-6.
978   92.   Yu G, Wang LG, He QY. ChIPseeker: an R/Bioconductor package for ChIP peak
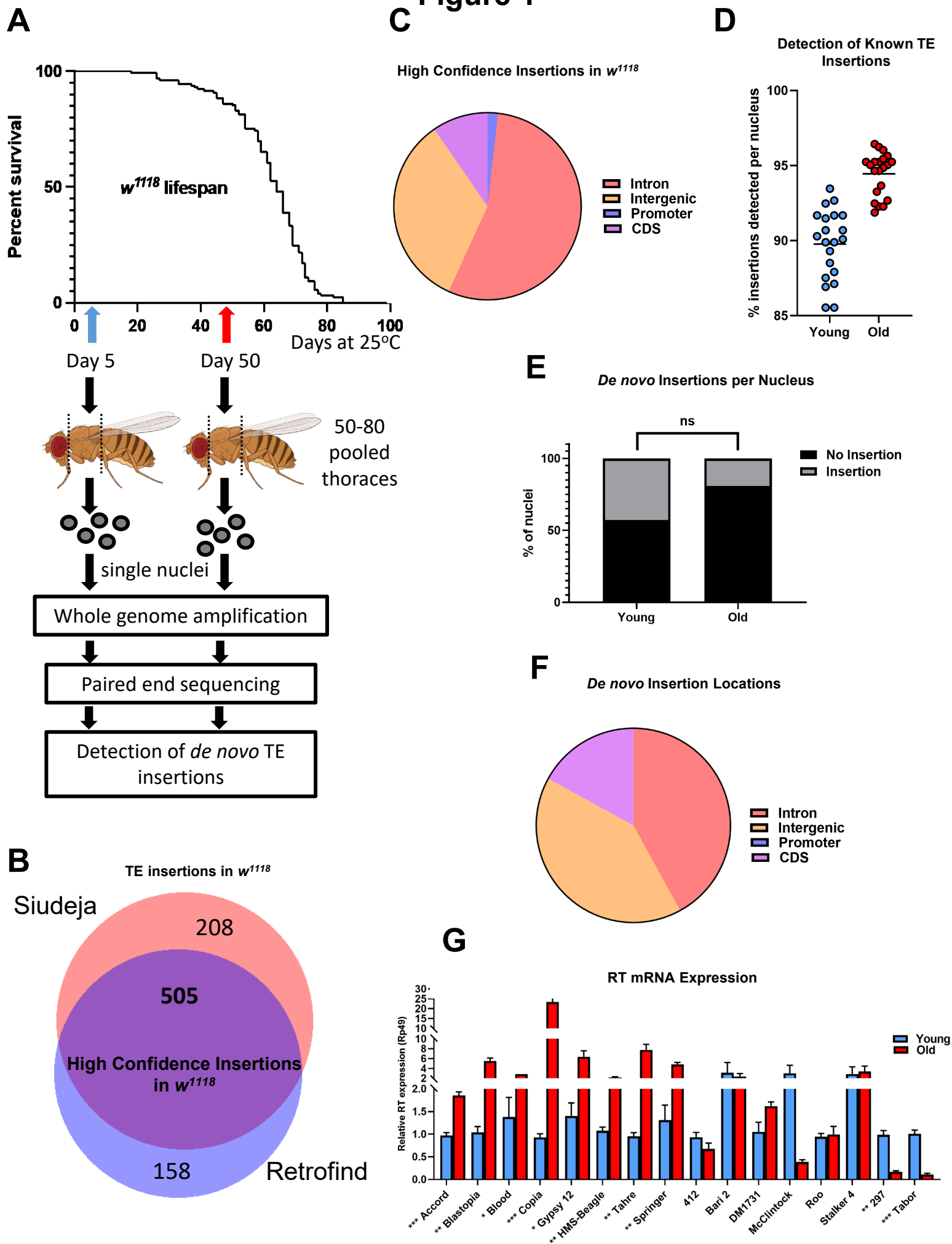979   annotation, comparison and visualization. Bioinformatics. 2015;31(14):2382-3.
980

Figure 1

A

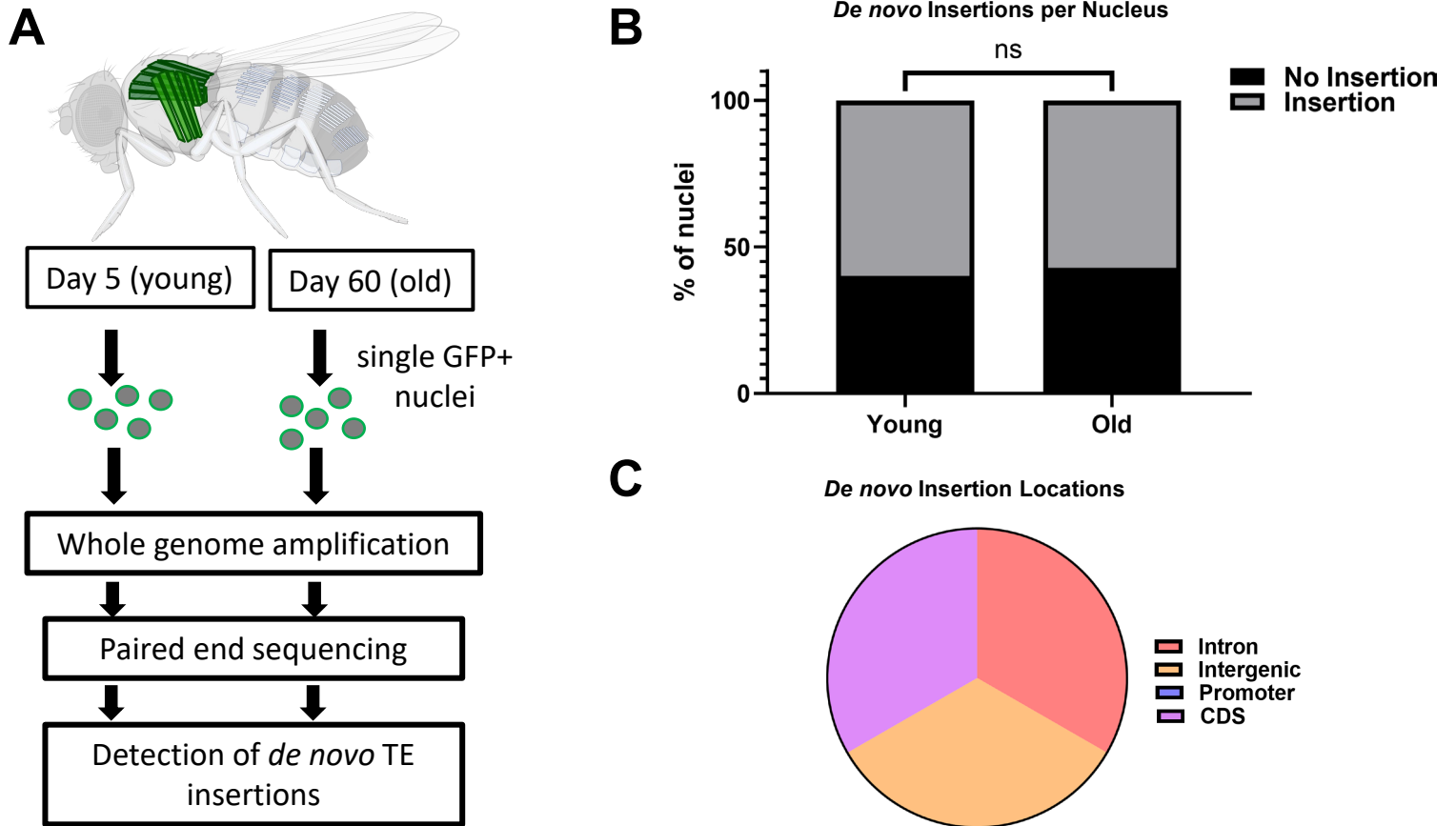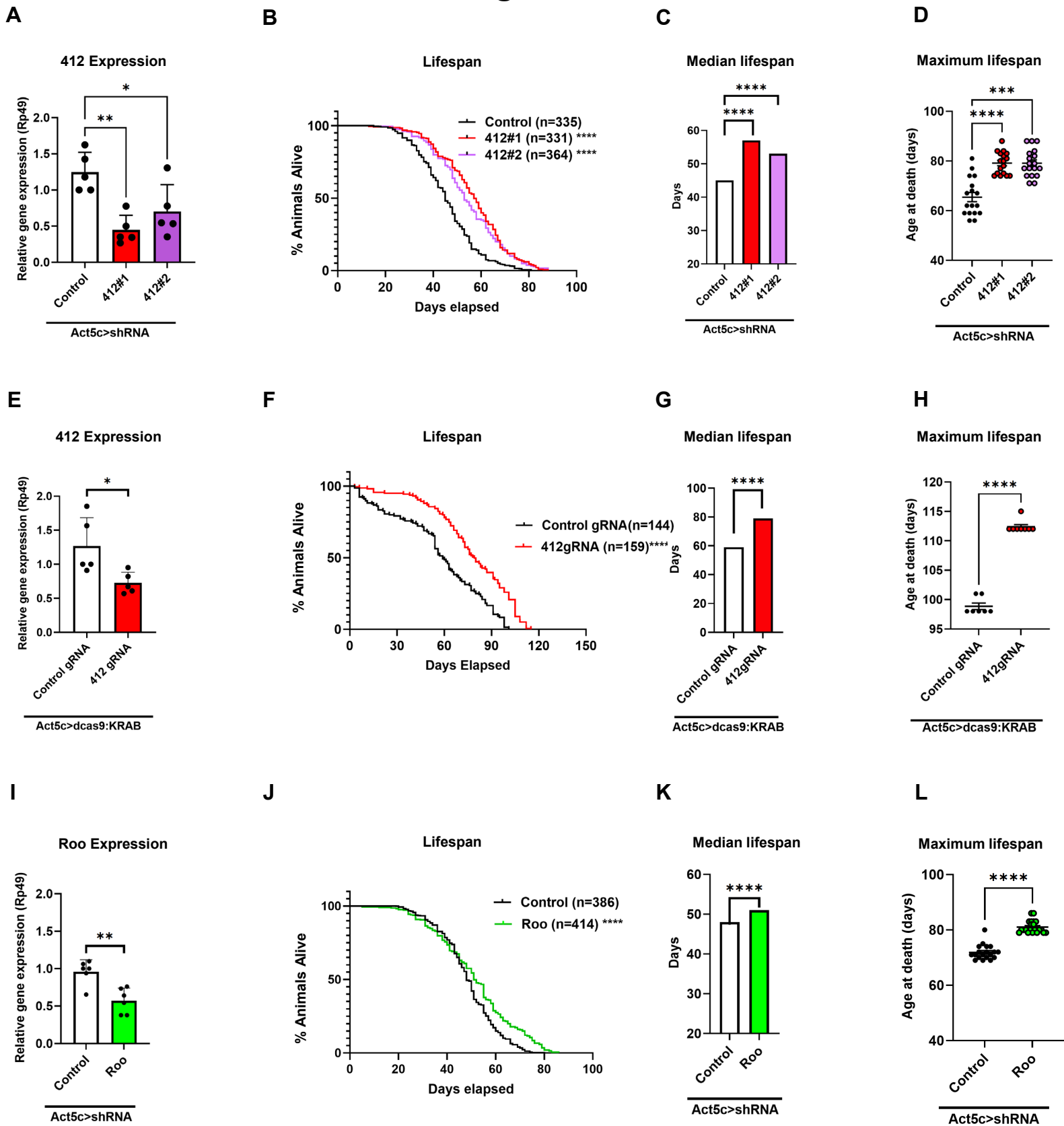

w^{1118} lifespan

Day 5

Day 50

50-80 pooled thoraces

single nuclei

Whole genome amplification

Paired end sequencing

Detection of *de novo* TE insertions

B

TE insertions in w^{1118}

Siudeja

208

505

High Confidence Insertions in w^{1118}

158

Retrofind

C

High Confidence Insertions in w^{1118}

- Intron
- Intergenic
- Promoter
- CDS

D

Detection of Known TE Insertions

% insertions detected per nucleus

Young   Old

E

De novo Insertions per Nucleus

ns

% of nuclei

- No Insertion
- Insertion

Young   Old

F

De novo Insertion Locations

- Intron
- Intergenic
- Promoter
- CDS

G

RT mRNA Expression

Relative RT expression (Rp49)

- Young
- Old

*** Accord, ** Blastopia, * Blood, *** Copia, * Gypsy 12, ** HMS-Beagle, ** Tahre, ** Springer, 412, Bari 2, DM1731, McClintock, Roo, Stalker 4, ** 297, *** Tabor

Figure 2

A

Day 5 (young)   Day 60 (old)

single GFP+ nuclei

Whole genome amplification

Paired end sequencing

Detection of *de novo* TE insertions

B

***De novo* Insertions per Nucleus**

ns

No Insertion
Insertion

% of nuclei

Young   Old
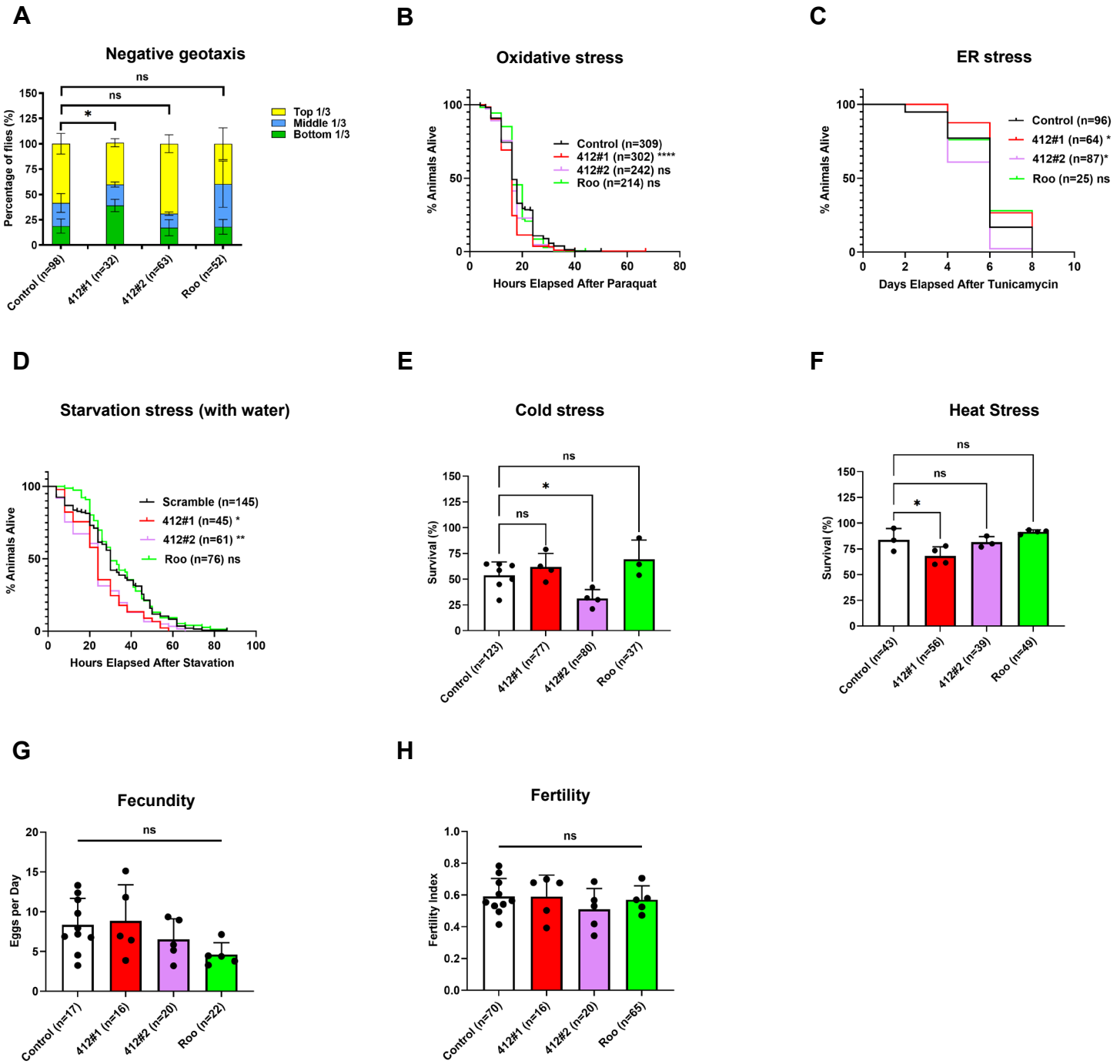
C

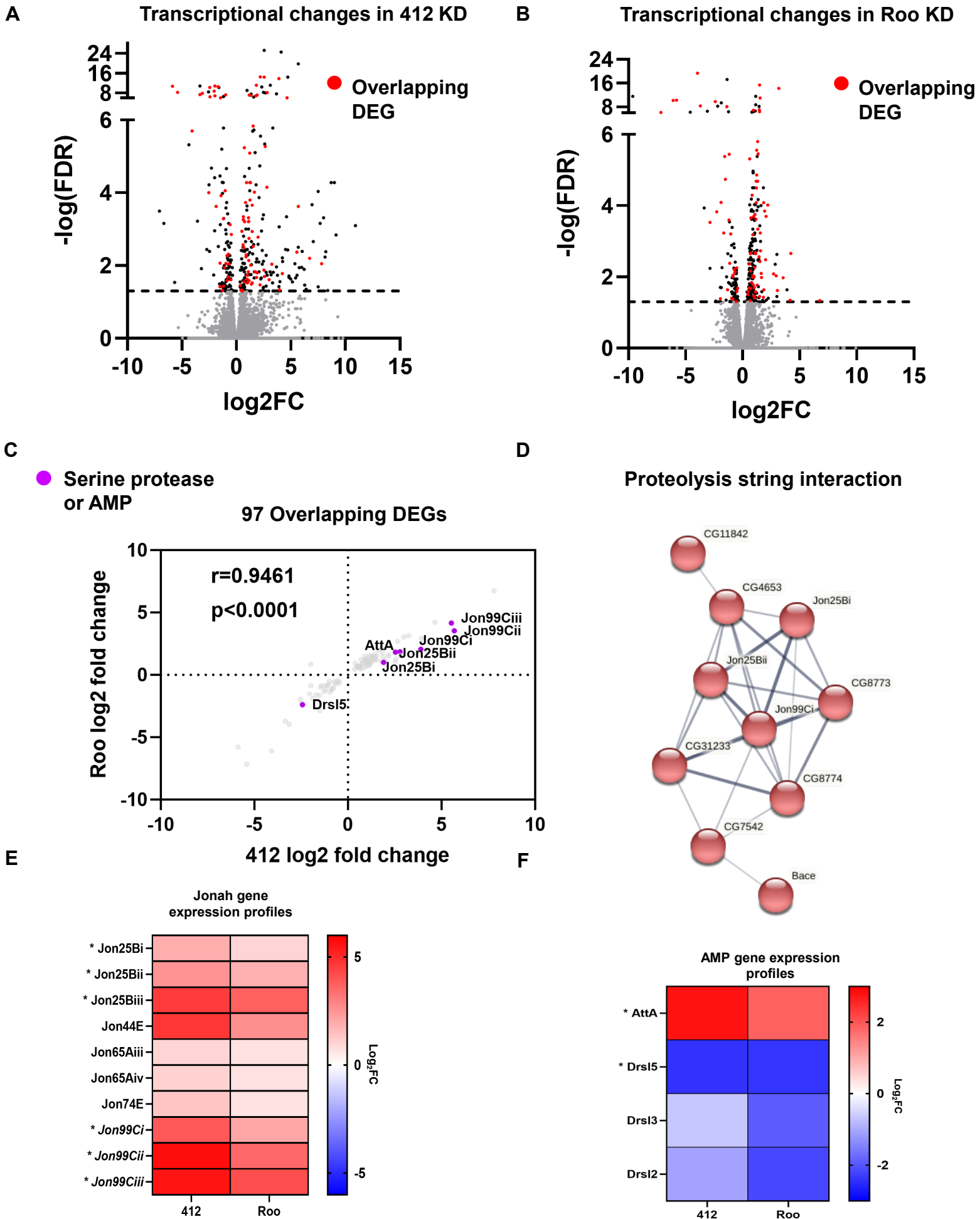***De novo* Insertion Locations**

Intron
Intergenic
Promoter
CDS

Figure 3

Figure 4

Figure 5

Supplemental Figure 1

Act5c>shRNA

A Control

B 412#1

C 412#2

D Roo

Act5c>dcas9-KRAB

E Control gRNA

F 412 gRNA
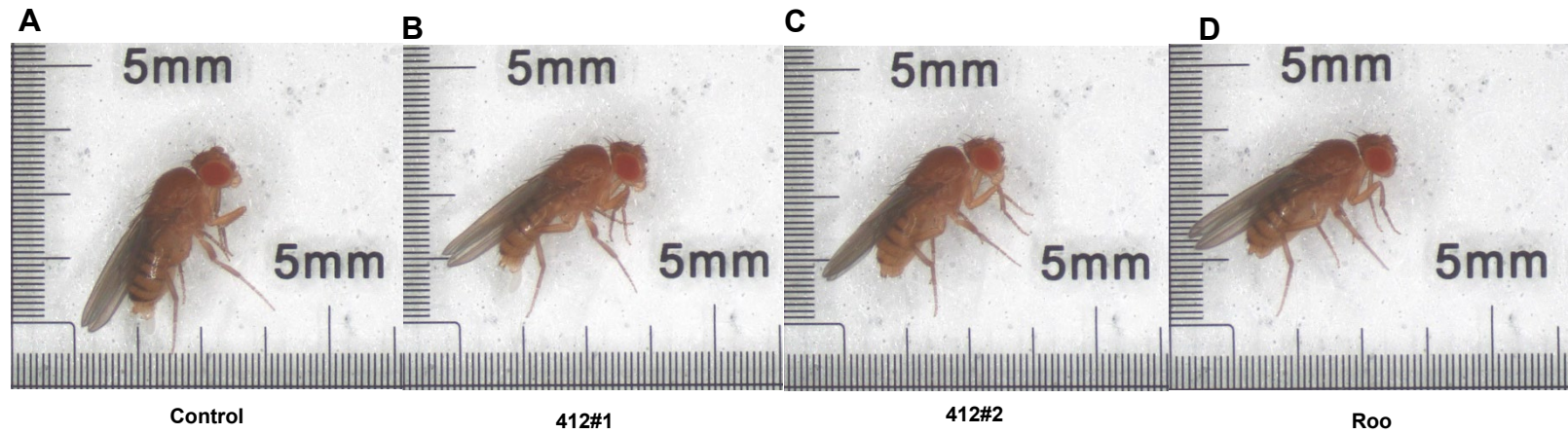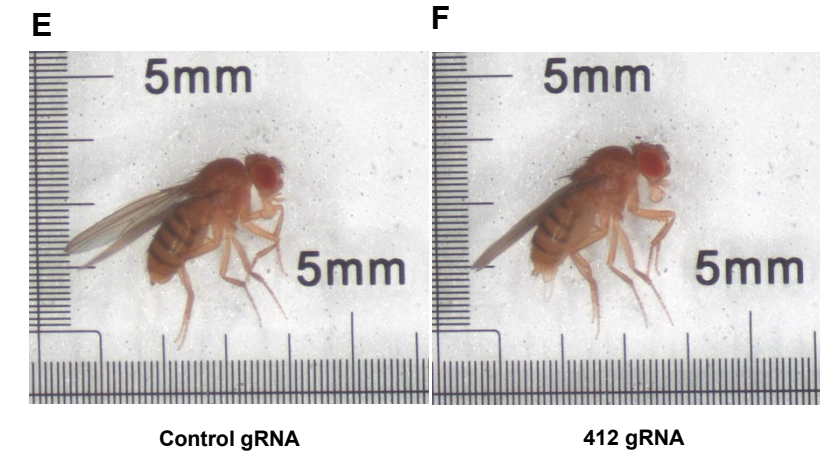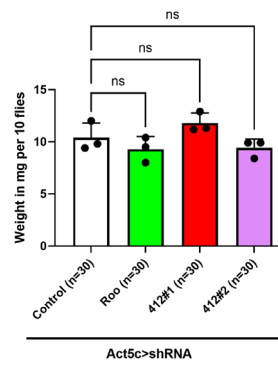
G Weight

H Weight
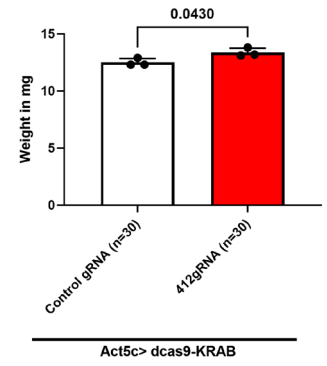
S1 Fig. Morphology and body weight of *412* and *Roo* knockdown animals

(A) Picture of the morphology of an Act5c>control shRNA fly. (B) Picture of the morphology of an Act5c>412#1 shRNA fly. (C) Picture of the morphology of an Act5c>412#2 shRNA fly. (D) Picture of the morphology of an Act5c>Roo shRNA fly. (E) Picture of the morphology of a CRISPRi (Act5c>dcas9-KRAB) with control gRNA fly. (F) Picture of the morphology of a CRISPRi (Act5c>dcas9-KRAB) with 412gRNA fly. (G) Body weight of Act5c>shRNA flies in milligrams (mg) per 10 flies. Each dot represents a set of 10 flies. This experiment was done in triplicate. One-way ANOVA. ns (412#1) p= 0.3535. ns (412#2) p= 0.5904. ns (Roo) p= 0.5250. (H) Body weight of Act5c>dcas9-KRAB CRISPRi flies in milligrams (mg) per 10 flies. Each dot represents a set of 10 flies. This experiment was done in triplicate. Unpaired t-test. * p= 0.0430.

Supplemental Figure 2
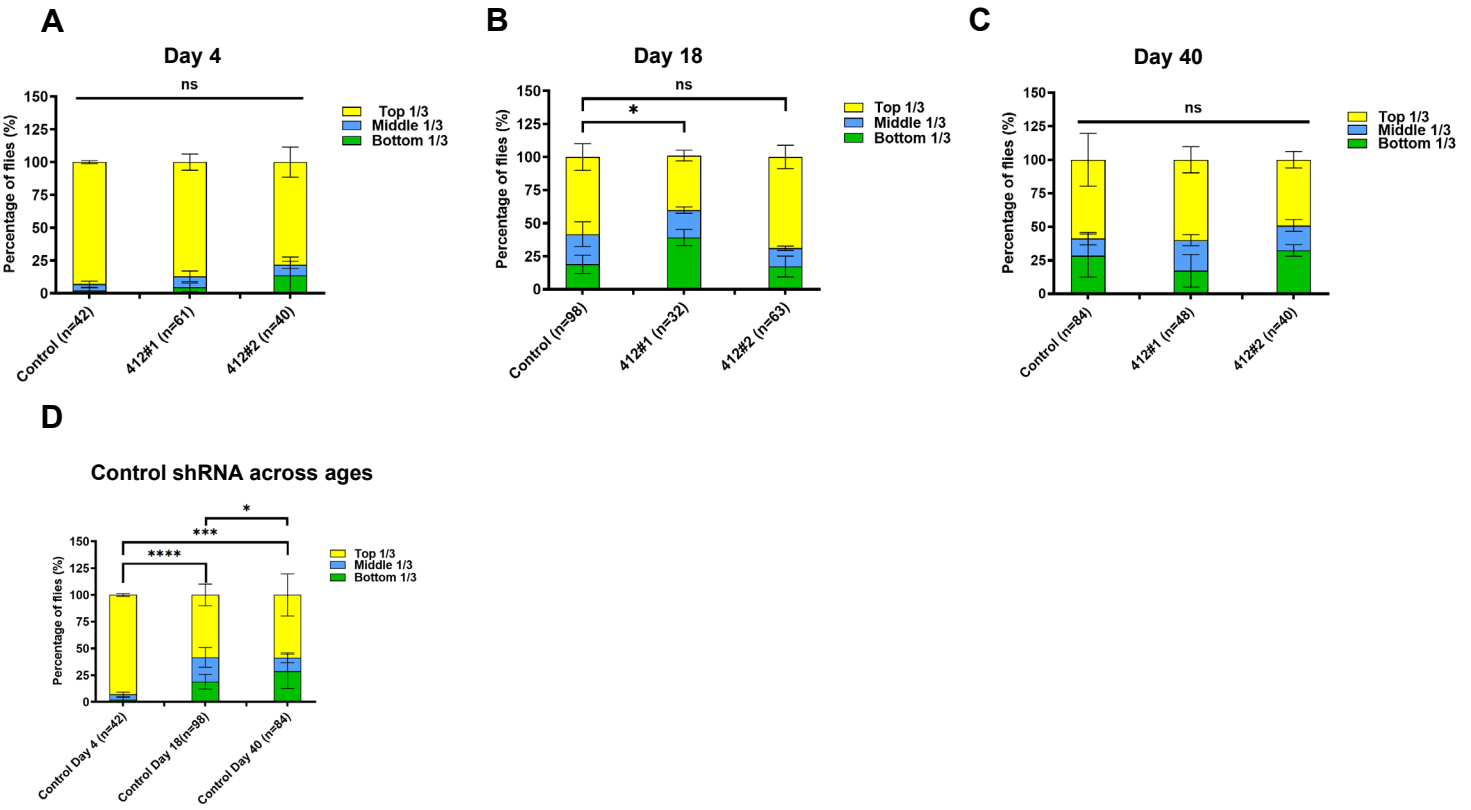
S2 Fig. Negative geotaxis locomotion assay across age

(A) Act5c>shRNA day 4 measurement of locomotion via negative geotaxis assay. The percentages of flies in each third of the vial is displayed. Fisher's exact test. ns (412#1) p= 0.5184. ns (412#2) p= 0.1119. (B) Act5c>shRNA day 18 measurement of locomotion via negative geotaxis assay. The percentages of flies in each third of the vial is displayed. Chi-square test for trend. * (412#1) p= 0.0332. ns (412#2) p= 0.4232. (C) Act5c>shRNA day 40 measurement of locomotion via negative geotaxis assay. The percentages of flies in each third of the vial is displayed. Chi-square test for trend. ns (412#1) p=0.4613. ns (412#2) p=0.3030. (D) Act5c>Control shRNA days 4, 20, and 40 measurement of locomotion via negative geotaxis assay. The percentages of flies in each third of the vial is displayed. Chi-square test for trend. **** (day 4 vs day 20) p<0.0001. *** (day 4 vs day 40) p= 0.0001. * (day 20 vs day 40) p= 0.0493.